A.I. Soler
Executive VP
Holtec International
Marlton, NJ

W.S. Hill
University of Pennsylvania
Philadelphia, PA

Effective Bending Properties for Stress Analysis of Rectangular Tubesheets[1]

The analysis of perforated plates has immediate application to tubesheet design. However, successful tubesheet stress analysis requires knowledge of tubesheet elastic properties; considerable effort has therefore been directed toward their determination. The research effort to date has focused on triangular and square, fully packed tube arrays usually employed in circular tubesheets. In this paper, a simple analytical expression is proposed which is suitable for determination of the effective bending stiffness of a perforated plate having both fully packed and laned arrays. Using available data on triangular and square tube arrays, together with some additional test data on tube arrays in common use on large power plant condensers with rectangular tubesheets, it is shown that a simple analytical relationship for determination of required effective bending stiffness gives good agreement with available data.

Introduction

A problem of considerable importance in heat exchanger design is establishment of proper tubesheet thickness to withstand imposed loadings. Although simple empirical formulas exist for circular tubesheets [1],[2] considerable attention has been focused on design of circular tubesheets by rigorous theoretical analysis [2–8]. To successfully apply theoretical analyses to tubesheet design, effective elastic constants which simulate increased flexibility due to the perforations must be established; in early analytical work, this increased flexibility was incorporated by means of a deflection efficiency which reduced the plate bending stiffness [2–4]. Some attempt was made in these works to propose analytical formulations for deflection efficiency in terms of array geometry; it has, however, required considerable experimental and theoretical analysis [9–18] to reach the point where reliable data can be included in pressure vessel codes [19, 20] allowing determination of deflection efficiency for even a limited class of tube arrays. The cited works have concentrated on deducing effective elastic constants for diagonal and square tube arrays in circular tube sheets that are completely tubed; that is, for sheets that have at most an untubed rim. An excellent state of the art summary of the elastic design of circular tubesheets with completely filled tube arrays is contained in [21]. In recent years, some attention has been focused on determination of effective plastic properties of perforated plates [22–24]; again, the configurations studied imply application to the circular tubesheet with a completely filled tube array.

The emphasis on design of tubesheets for round heat exchangers is understandable in light of the variety of high pressure, high temperature, and corrosive environments that these units may encounter in different services. The design of rectangular tubesheets for large power plant condensers has only recently begun to receive some attention [8, 25, 26]. This seeming lack of attention to tubesheet design in rectangular heat exchange units, now running to over 1,000,000 sq ft (9.29×10^4 m^2) of condensing surface, is readily explained. Until recently, the majority of condenser cooling water units used "siphon circuits" with very low tubesheet pressures; these low design pressures allowed employment of a standard minimum thickness tubesheet without extensive design effort. With increased use of cooling tower circuits, however, condenser water pressures have risen to 50–150 psi (345–1034 Pa); careful consideration of proper tubesheet thickness

---

[1] "LEGAL NOTICE"—This work was prepared by (University of Pennsylvania) as an account of work sponsored by the Electric Power Research Institute, Inc. ("EPRI"). Neither EPRI, members of EPRI, nor (University of Pennsylvania), nor any person acting on behalf of either:

"(*a*) Makes any warranty or representation, express or implied, with respect to the accuracy, completeness, or usefulness of the information contained in this report, or that the use of any information, apparatus, method, or process disclosed in this report may not infringe privately owned rights; or

"(*b*) Assumes any liabilities with respect to the use of, or for damages resulting from the use of, any information, apparatus, methods or process disclosed in this report."

[2] Numbers in brackets designate References at end of paper.

Contributed by the Power Division and presented at the Winter Annual Meeting, New York, N. Y., December 5–10, 1976, of THE AMERICAN SOCIETY OF MECHANICAL ENGINEERS. Manuscript received at ASME Headquarters April 8, 1976. Paper No. 76-WA/Pwr-1.

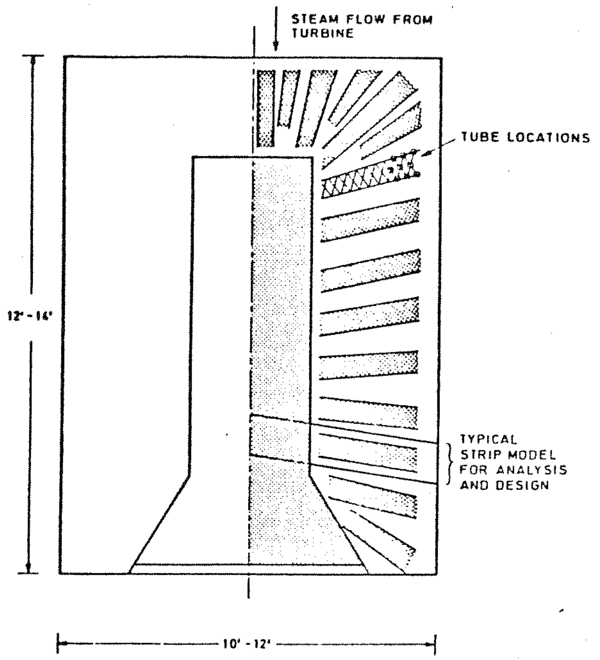

Fig. 1 Typical rectangular tubesheet for large power plant condenser

is required because of the large planform areas involved, and because of large moments and forces which may be imposed on the tubesheets from external piping. Reference [25] contains a qualitative discussion of the power plant condenser tubesheet design problem, including loadings, and contains some results generated from a computer approach to the establishment of proper tubesheet thickness.

Determination of effective constants for rectangular power plant condenser tubesheets is more involved than a similar determination for circular tubesheets because the array geometry varies over the entire tubesheet. Fig. 1 (not to scale) shows a typical arrangement with certain lanes of tubes removed to promote a uniform distribution of steam to the inner portion of the tube bundle. This creates a "spider web" or "laned" configuration of tubes around much of the periphery. The tubesheet essentially has a variable effective elastic bending stiffness depending on the location considered. Reference [25] also contains a figure showing a typical large condenser tubesheet. The tubesheet loading and load transfer mechanism is adequately discussed in [25]; for the purposes of the work herein, it suffices to say that current industry design philosophy considers typical strips of the condenser tubesheet oriented from the edge of the tubesheet in toward the center and establishes tubesheet thickness from analysis of one or more strips with the highest loading. Inherent in this simplified analysis, such as described in [8], is the assumption that the tubesheet sections deform as individual strips on elastic foundations; such an assumption is reasonable except near corners of the sheet, and in any event, must be employed if any simple formulation is to be achieved.

It is not readily apparent that the considerable data amassed for fully packed tube arrays can be directly applied to the analysis of condenser tubesheets with laned arrays. It is the purpose of this paper to establish a procedure for simple determination of the effective bending rigidity of rectangular tubesheets with the various kinds of tube arrays found in large condensers.

Data Analysis and Results

Figs. 2(a), 2(b), and 2(c) show typical tube layouts for sections of modern power plant condensers. The diagonal array of Fig. 2(a) has been well studied in the literature. Rectangular and laned arrays are commonly used in condenser design to afford additional passageway for the steam flow to the center of the tube bundle. Anticipating application to a strip type of deformation analysis, we show in Fig. 2 the width of strip b, representing a repeating section, which forms the basis of the strip model. Herein, we consider the determination of effective elastic constants for the typical strips shown. The assumption of cylindrical bending for each strip allows consideration of only a single strip and includes the Poisson effect only as it contributes to the plate bending stiffness $Et^3/12(1-\nu^2)$.

Fig. 3 shows the simple experimental arrangement set up to measure the effect of perforations. Steel strips obtained from standard stock were used as test specimens. All tests were carried out using $1 \times 24 \times 0.25$ in. ($2.54 \times 60.96 \times 0.635$ cm) strips. Application of dead weight loading produced a measurable central deflection so that an elastic load deflection curve was easily obtained for each strip tested. Several loads were used to establish each load deflection curve. Tests were performed on undrilled specimens and on specimens drilled to various perforation configurations. Since only the deflection ratio (drilled specimen to undrilled specimen) was desired, the problem of establishing particular boundary conditions did not arise. As long as the support points and the clamp location were identical in both the undrilled and the drilled test piece, an accurate measure of the weakening effect of the perforations was easily obtained. Table 1 shows the configurations studied experimentally.

We now consider the foregoing data and much of the valid data already reported on in previous works. Figs. 4 and 5 show a plot of deflection efficiency b^*/b ($= D^*/D$) versus ligament efficiency h/P where ligament width h = tube pitch P − hole diameter. The quantity b^* may be considered as an effective width (less than b) which represents the weakening effect of the perforations. The concept of an effective width in this strip application is equivalent to assuming an effective bending stiffness D^*/D. Plotted in Figs. 4 and 5 are data obtained from [8, 15, 18, 19, 20]. The data in [18, 19] gave E^*/E and ν^* separately which permit calculation of $D^*/D = (E^*/E)(1-\nu^2)/(1-\nu^{*2})$. Also plotted on Fig. 4 are our experimental results on 30 deg diagonal array configurations. We must recognize, however, that the results obtained using the test set up of Fig. 3 contain some influence of anti-clastic curvature, and, therefore, probably represent the ratio E^*/E rather than D^*/D. We shall comment more on this later; for the present we plot our data directly on Fig. 4. The solid bounding curves in Figs. 4 and 5 represent results obtained from an assumed analytical description which we put forth as the major contribution of this work. That is, the results plotted show that it is possible to develop a useful formula relating D^*/D to ligament efficiency. In [16, 21] it was noted that the deflection efficiency, D^*/D is strongly dependent on the "solidity factor" of the plate; that is, if the solidity factor f of the perforated segment is defined as

Nomenclature

b = width of strip for analysis

b^* = effective width of strip accounting for perforations

t, E, ν = tubesheet thickness, Young's modulus, Poisson's ratio

$D = Et^3/12(1-\nu^2)$ = plate bending stiffness

D^* = effective plate bending stiffness

P = tube pitch (Fig. 2)

h = ligament width = tube pitch − tube OD

f = solidity (defined by equation (1))

ϕ = thickness coefficient (defined by equation (5))

λ = coefficient (defined by equation (6))

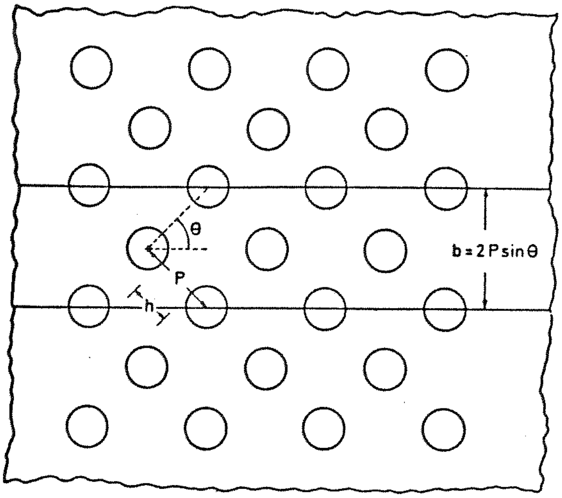

Fig. 2(a) Tube layout, diagonal array θ = 30, and 60 deg, square array θ = 45 deg

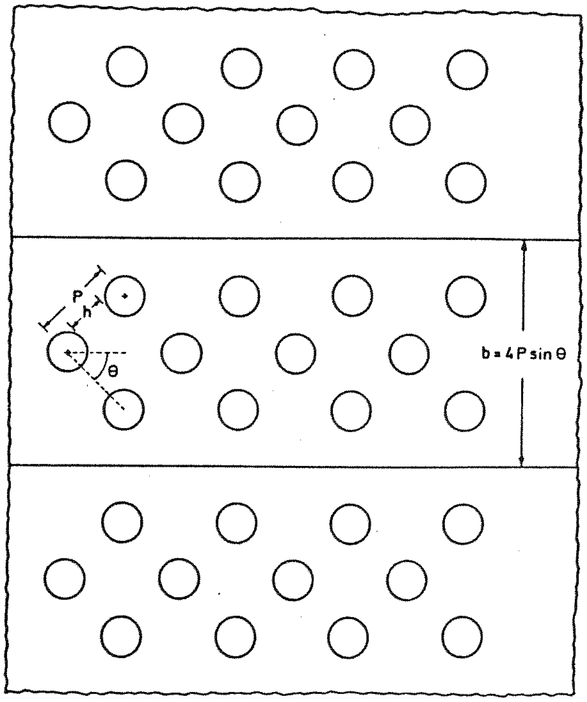

Fig. 2(c) Tube layout, laned array

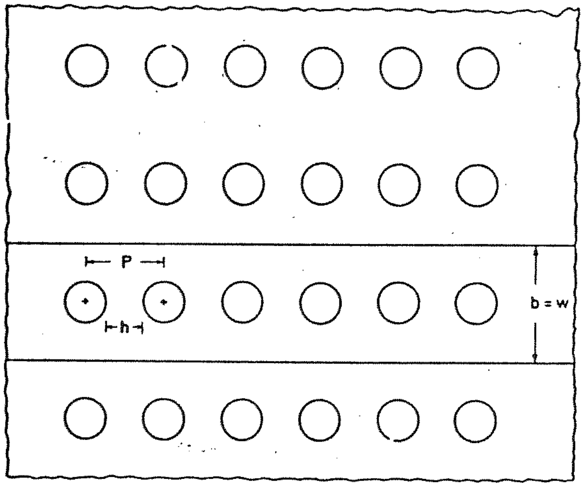

Fig. 2(b) Tube layout, rectangular array (square pitch $b = P$)

$$f = \frac{\text{metal area after drilling}}{\text{metal area before drilling}}; \quad 0 < f \leq 1 \tag{1}$$

then it appears that for a given thickness plate

$$D^*/D = \text{function of solidity factor } f \tag{2}$$

regardless of particular array configuration. The ligament efficiency h/P enters into equation (2) initially by virtue of the dependence of f on h/P. This relationship between D^*/D and f was recognized by Miller [4] who assumed that

$$D^*/D = f \tag{3}$$

Although equation (3) is not plotted in Figs. 4 and 5, it can easily be shown to predict ratios b^*/b (or D^*/D) that are significantly larger than the experimental results, especially for the smaller h/P ratios representative of practical condenser tubesheets. Examination of all of the data plotted in Figs. 4 and 5 indicated that bounding equations that gave a good fit, within experimental error, to the plotted data could be obtained in the form

$$\frac{b^*}{b} = \frac{D^*}{D} = f^\lambda; \quad \lambda = \lambda\left(\frac{h}{P}, \frac{t}{2P}\right) \tag{4}$$

where t = plate thickness. Specifically, if we define a thickness coefficient ϕ

$$\phi = \left(\frac{t}{2P} - 1\right) \Big/ \left(\frac{t}{2P} + 1\right) \tag{5}$$

then the complete range of plate thickness variations is described by $-1 \leq \phi \leq 1$. We note that the dividing line between thin plates and thick plates is defined in [19, 20] as $t/2P = 1$, or $\phi = 0$. We propose, based on the examined data, and a series of curve fittings, etc., to specify the function λ to be used in equation (4) as

$$\lambda = \frac{13 + 3\phi}{8}\left[1 + \frac{(3 - \phi)}{4}\frac{h}{P} + \frac{(1 + \phi)}{2}\frac{h}{P}\left(1 - \frac{h}{P}\right)^2\right] \tag{6}$$

By way of reference, we note that the solidity factor f for the configurations of Figs. 2(a), 2(b), and 2(c) are easily obtained in the form:

$$f = \left[1 - \frac{\pi}{4\sin 2\theta}\left(1 - \frac{h}{P}\right)^2\right] \text{(Fig. 2(}a\text{))} \tag{7}$$

$$f = \left[1 - \frac{\pi P}{4w}\left(1 - \frac{h}{P}\right)^2\right] \text{(Fig. 2(}b\text{))} \tag{8}$$

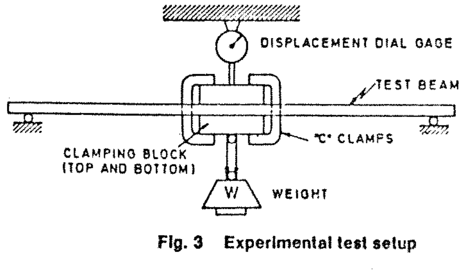

Fig. 3 Experimental test setup

$$f = \left[1 - \frac{3\pi}{16}\frac{(1 - h/P)^2}{\sin 2\theta}\right] \text{(Fig. 2}(c)\text{)} \tag{9}$$

The bounding curves in Figs. 4 and 5 were constructed using equations (4)–(7) and represent a simple analytical formulation which gives good agreement with the available data for fully packed arrays. We must note, however, that equation (6) was formulated by simple trial and error techniques, so that it is quite probable that other curve fitting techniques than were used could give a different representation that would equally well bound the available data. It should be pointed out that the large spread in the plotted data points is apparently due to the thickness parameter ϕ. We have plotted in Figs. 4, 5, and 6 bounding curves for very thick plates ($\phi = 1$), and for very thin plates ($\phi = -1$). The location of experimental data points between these bounding curves reflects the actual $t/2P$ value used in the previously reported experiments. The data points representing experimental work performed during this research effort give results in reasonable correlation with the suggested thickness parameter ϕ (i.e., $t/2P = 0.125$, $\phi = -0.78$ for our points plotted in Fig. 4; $t/2P = 0.289$, $\phi = -0.552$ for the rectangular array in Fig. 6; and, $t/2P = 0.433$, $\phi = -0.396$ for the laned array in Fig. 6). We still feel confident in proposing equation (6) as a useful representation, especially in view of the success obtained using it to construct the bounding curves, in Fig. 6, for tests of the laned array configurations of Figs. 2(b) and Fig. 2(c) where the arrays are not fully packed. No other data exist for these configurations save the results obtained in this work using the test set up described earlier.

Fig. 6 shows a comparison between the predictions based on equations (4)–(6) applied to the solidity factors of equations (8) and (9), and the limited experimental data obtained from our strip tests. The solid lines show the bounding curves for $\phi = \pm 1$, while the dotted curve shows the prediction obtained using the ϕ value appropriate

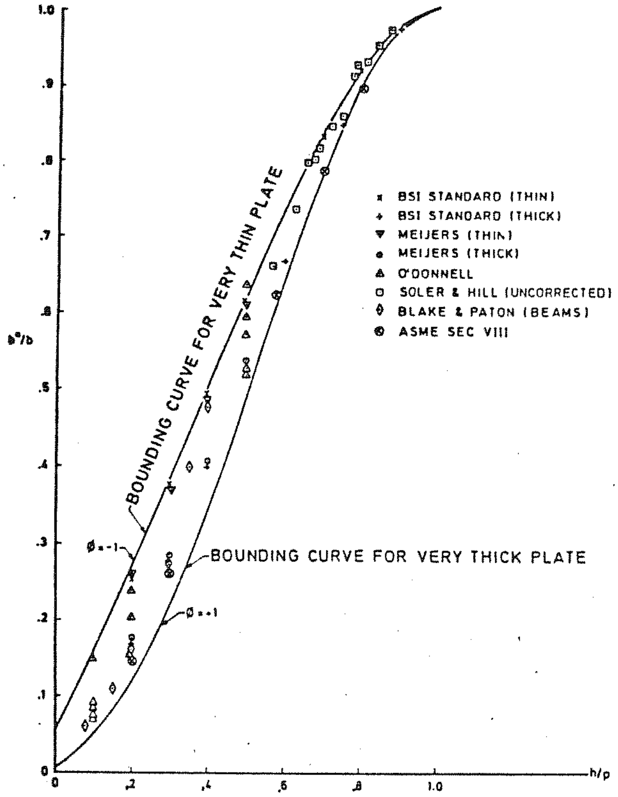

Fig. 4 Deflection efficiency versus h/P diagonal pitch

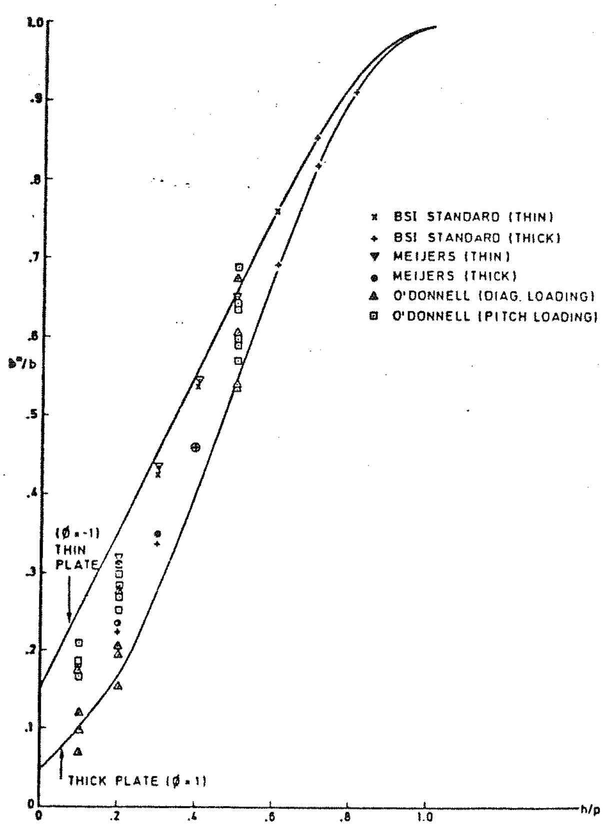

Fig. 5 Deflection efficiency versus h/P square pitch

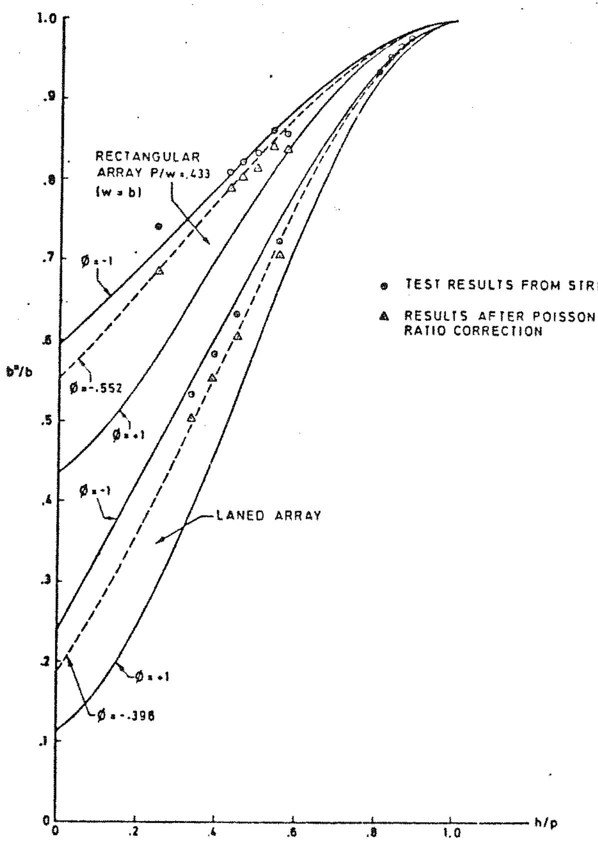

Fig. 6 Deflection efficiency versus h/P single row and laned section

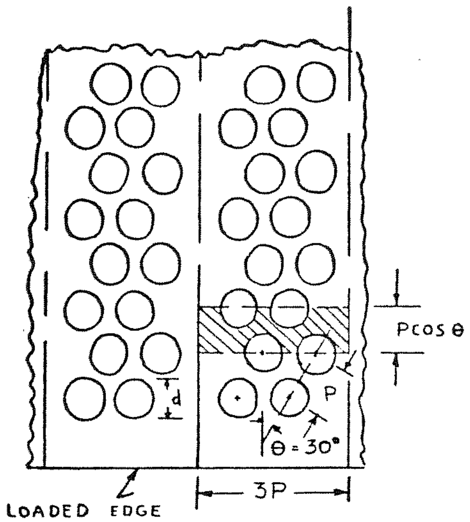

Fig. 7 Tube layout for sample design calculation

to the actual strip tested. Note that in Fig. 6 we have plotted the experimental points obtained directly from the test data (that is, assuming the test data directly gave the ratio $b^*/b = D^*/D$), and also a set of points obtained by correcting the test data for Poisson effects (anti-clastic curvature) that are probably present because of the dimensions of our test strips. The initial set of experimental points, obtained directly from the test data, appears to indicate that use of the proposed λ relationship (equation)6)) underestimates the deflection efficiency, especially for smaller h/P ratios. However, if one realizes that the test data are more realistically a measure of E^*/E, rather than D^*/D (because a beam strip was tested without any precautions taken to eliminate anti-clastic curvature), then it is appropriate to correct our test data by multiplying by the factor $(1 - \nu^2)/(1 - \nu^{*2})$ in order to more fairly test the predictions of our proposed analytical formulation. This modification to our test results could only be done approximately since our test set up did not lend itself to any direct accurate measurement of ν^*, the effective Poisson's ratio.

To obtain a first approximation of the possible magnitude of the correction, we proceeded in the following manner. We applied the Poisson correction to the data obtained from testing the rectangular array by using the effective Poisson's ratio ν^* for the square array given in [18, 20]. We corrected the raw test data for the laned array by using an effective Poisson's ratio arbitrarily computed as the average between 0.3 for an unperforated strip and the value of ν^* taken from [18, 20] for a fully perforated diagonal array. The average value was used since there is a considerable amount of undrilled plate in the repeated section making up the laned array. Applying the indicated Poisson's ratio correction to our test data gives what we feel is a better representation of the deflection efficiency for the arrays under consideration, and indeed, these corrected points plotted in Fig. 6 indicate that the proposed analytical representation will give a good representation of the proper deflection efficiency. The four experimental test points plotted in the range $h/P \approx 0.800$ in Fig. 6 reflects a series of early tests performed on a rectangular array with $P/w = 0.866$. The theoretical formula indicates that the solidity of such a section is numerically almost identical to that of the laned array. There are, however, slight differences in the function λ because of the different values of ϕ.

Typical Design Calculation

As an application of the formulas developed herein, we determine the effective bending modulus D^* for the configuration shown in Fig. 7 where a laned array has been formed by eliminating every third tube hole in rows parallel to the edge. Assuming that the arrangement

Table 1 Configuration tested

Type	Hole Diameter	Pitch	Ligament/Pitch
1. Undrilled	———	—	———
2. 30° diagonal (Fig. 2A)	1/8" (3.175 mm)	1"	.875
	5/32" (3.969 mm)		.844
	3/16" (4.763 mm)		.813
	7/32" (5.556 mm)		.781
	1/4" (6.35 mm)		.750
	9/32" (7.14 mm)		.719
	5/16" (7.94 mm)		.688
	11/32" (8.73 mm)		.656
	3/8" (9.53 mm)		.625
3. Rectangular (Fig. 2B) w = 1"	3/16" (4.763 mm)	.433	.567
	13/64" (5.159 mm)		.531
	7/32" (5.556 mm)		.495
	15/64" (5.953 mm)		.459
	1/4" (6.35 mm)		.423
	21/64" (8.33 mm)		.242
	1/8" (3.175 mm)	.866	.856
	9/64" (3.572 mm)		.838
	5/32" (3.969 mm)		.820
	3/16" (4.763 mm)		.783
4. Laned (Fig. 2C)	1/8" (3.175 mm)	.2887	.567
	5/32" (3.969 mm)		.459
	11/64" (4.366 mm)		.405
	3/16" (4.763 mm)		.351

shown is repeated, we now establish the modulus D^* appropriate to the repeated width of strip $3P$. Fig. 7 indicates that the undrilled representative area is

$$A_{ud} = 3P \times P \cos\theta \tag{10}$$

The representative area after drilling is given as

$$A_D = A_{ud} - 4\left(\frac{\pi d^2}{8}\right) \tag{11}$$

so that the solidity f is given as

$$f = \frac{A_d}{A_{ud}} = 1 - \frac{\pi}{6}\frac{d^2}{P^2 \cos\theta} \tag{12}$$

We consider, for example,

$$d/P = 1.0/1.25 = 0.8 \tag{13}$$

which implies a ligament efficiency h/P as

$$h/P = 1 - d/P = 0.2 \tag{14}$$

For this configuration, with $\theta = 30$ deg, we obtain

$$f = 0.613 \tag{15}$$

Assuming that the thickness of the plate is such that $t/2P = 0.5$ leads us to a results for the parameter ϕ (equation (5)) as

$$\phi = -1/3 \tag{16}$$

Using equations (14) and (16) in equation (6) then yields

$$\lambda = 1.739 \tag{17}$$

so that

$$D^*/D = (0.613)^{1.739} = 0.427 \tag{18}$$

which suggests that the effective bending modulus has been reduced to 42.7 percent of the modulus for the corresponding homogeneous plate for this set of parameters.

Summary

An examination of available experimental data plus additional data obtained during this study has enabled us to propose an analytical formulation for the effective bending stiffness of a perforated strip. The major contribution of this work is the development of the analytical formulation which can be extended to any tube array geometry which is encountered when a strip analysis of a rectangular condenser tubesheet is undertaken.

References

1 Standards of the Tubular Exchanger Manufacturer's Association, TEMA. New York, N. Y., 1968.

2 Gardner, K. A., "Heat Exchanger Tube Sheet Design," TRANS. ASME, Vol. 70, 1948, pp. A-377-385.

3 Gardner, K. A., "Heat Exchanger Tube Sheet Design—2: Fixed Tube Sheets," TRANS. ASME, Vol. 74, 1952, pp. A-159-166.

4 Miller, K. A. G., "Design of Tube Plates in Heat Exchangers," *Proc. Inst. Mech. Eng.*, Series B, Vol. 1, 1952, pp. 215-231.

5 Boon, G. B., and Walsh, R. A., "Fixed Tubesheet Heat Exchangers," *Journal of Applied Mechanics*, TRANS. ASME, Series E, Vol. 86, 1964, pp. 175-180.

6 Gardner, K. A., "Heat Exchanger Tubesheet Design 3: U-tube and Bayonet Tube Sheets," *Journal of Applied Mechanics*, TRANS. ASME, Series E, Vol. 82, 1960, pp. 25-32.

7 Yu, Y. Y., "Rational Analysis of Heat Exchanger Tubesheet Stresses," TRANS. ASME, Vol. 78, 1956, pp. A-468-473.

8 Blake, C. S., and Paton, A. D., "Design of Rectangular Tubeplates for Large Heat Exchangers," *Journ. Mech. Eng. Science*, Vol. 5, No. 3, 1963, pp. 211-226.

9 Malkin, I., "Notes on a Theoretical Basis for the Design of Tubesheets of Triangular Layout," TRANS. ASME, Vol. 74, 1952, pp. 387-396.

10 Horvay, G., "Bending of Honeycombs and Perforated Plates," TRANS. ASME, Vol. 74, 1952, pp. A-122-123.

11 Bailey, R., and Hicks, R., "Behavior of Perforated Plates Under Plane Stress," *Journal of Mechanical Engineering Science*, Vol. 2, No. 2, 1960.

12 Duncan, J. P., and Upfold, R. W., "Equivalent Elastic Properties of Perforated Bars and Plates," *Journ. of Mech. Eng. Science*, Vol. 5, No. 1, 1963.

13 Slot, T., and Yalch, J. P., "Stress Analysis of Plane Perforated Structures by Point-Wise Matching of Boundary Conditions," *Nuclear Engineering and Design*, Vol. 4, No. 2, Aug. 1966.

14 Goldberg, J E., and Jabbour, K. N., "Stresses and Displacements in Perforated Plates," *Nuclear Structural Engineering*, No. 2, 1965, pp. 360-381.

15 Meijers, P., "Doubly Periodic Stress Distributions in Perforated Plates," PhD thesis, University of Delft, Holland, 1967.

16 Meijers, P., "Plates With a Doubly Periodic Pattern of Circular Holes Loaded in Plane Stress or in Bending," First International Conference on Pressure Vessels Technology, Part I, Design and Analysis, 1969.

17 Slot, T., and O'Donnell, W. J., "Effective Elastic Constants for Thick Perforated Plates With Square and Triangular Penetration Patterns," *Journal of Engineering for Industry*, TRANS. ASME, Series B, Vol. 93, No. 4, Nov. 1971, pp. 935-942.

18 O'Donnell, W. J., "Effective Elastic Constants for Bending of Thin Perforated Plates With Triangular and Square Penetration Patterns," *Journal of Engineering for Power* TRANS. ASME, Series B, Vol. 95, Feb. 1973, pp. 121-128.

19 ASME Boiler and Pressure Vessel Code, Section III; Section VIII, Div. 2, New York, New York, 1974.

20 BSI Committee document 75/72860, June 1975.

21 Gardner, K. A., "Tubesheet Design: A Basis for Standardization," *Proceedings of the First International Conference on Pressure Vessel Technology: Part I, Design & Analysis*, ASME, N. Y., 1969, pp. 621-648.

22 O'Donnell, W. J., and Porowski, J., "Yield Surfaces for Perforated Materials," *Journal of Applied Mechanics*, Mar. 1972, pp. 263-270.

23 Porowski, J., and O'Donnell, W. J., "Effective Plastic Constants for Perforated Materials," *Journal of Pressure Vessel Technology*, TRANS. ASME, Series J, Vol. 96, No. 3, Aug. 1974, pp. 234-241.

24 Porowski, J., and O'Donnell, W. J., "Plastic Strength of Perforated Plates With Square Penetration Patterns," ASME Paper No. 75-PVP-9, presented at 1975 Pressure Vessel and Piping Technology Conference, San Francisco, 1975.

25 Peake, C. C., Gerstenkon, G. F., and Arnold, T. R., "Some Reliability Considerations-Large Surface Condensers," presented at 1975 American Power Conference, Chicago, Ill., Apr. 1975.